Improved Wave Force Classification Using System Identification

P K Stansby, K Worden and G R Tomlinson
Department of Engineering
University of Manchester
Oxford Road
Manchester
M13 9PL

S A Billings
Department of Automatic Control and Systems Engineering
University of Sheffield
P O Box 600
Mappin Street
Sheffield
S1 4DU

Research Report No 440

October 1991

Improved Wave Force Classification Using System Identification

P.K.Stansby, K.Worden and G.R.Tomlinson
Department of Engineering
The University
Oxford Road
Manchester M13 9PL

S.A.Billings
Department of Automatic Control and Systems Engineering
University of Sheffield
Mappin Street
Sheffield S1 3JD

Abstract

An extension to the Morison equation including Duffing-oscillator type force terms is postulated through knowledge of the flow mechanisms. This is used to curve fit measured force time-histories from velocity time-histories, generated experimentally from various sources: regular oscillatory flow in a U-tube, cylinder oscillation in still water and in a current, random waves in the large De Voorst wave flume and a directional sea state at the Christchurch Bay Tower. The curve fits from the Morison equation are sometimes poor while the curve fits from the extended equation are always excellent, although the corresponding 'predictions' give little or no improvement on the Morison equation. The curve fits obtained by simply adding a term proportional to $F|F|$, where F is force, are also significant improvements over the Morison fits enabling an improved classification of force in terms of drag, inertia and history (for each flow situation). In unidirectional flows the association of a significant history term with vortex shedding is confirmed by the occurrence of a prominent transverse or lift force. In directional seas, lift (due to vortex shedding) cannot be isolated and it is suggested that the data analysis described here will indicate the significance of vortex shedding through the relative magnitude of the history term.

1 Introduction

Since its introduction in 1950 [1], the Morison equation has provided the main means of predicting wave forces on slender cylinders. In the usual notation,

$$\frac{\partial F}{\partial l} = \frac{1}{2}\rho D C_d u|u| + \frac{1}{4}\pi\rho D^2 C_m \dot{u} \tag{1}$$

where $u(t)$ is the instantaneous flow velocity, ρ is water density, D is diameter and l is axial length. The dimensionless drag and inertia coefficients C_d and C_m depend on the characteristics of the flow. In general the main dependence is taken to be on Re, the Reynolds number, and KC, the Keulegan-Carpenter number although these parameters do not have generally accepted definitions in random or directional waves. In place of Re, the Stokes parameter $\beta = Re/KC$ is often used. The coefficients C_d and C_m are usually obtained by applying least-squares procedures to measured force and velocity data.

The equation generally predicts the main trends in measured data quite well; however, some characteristics of the flow are not well represented. For example, in sinusoidal oscillatory flow the force variation at the fundamental frequency may be well predicted while that at higher harmonics is not. One result is that peak forces can be underpredicted. A poor representation of the high frequency content of the forces is a serious limitation for the determination of the fatigue life of a structural element.

One aim of the project was to determine whether the Morison equation may be extended to produce a better prediction of force time-histories measured in a variety of flow situations, ranging from sinusoidal flow in a U-tube, to unidirectional random waves in a large wave flume, to directional seas in Christchurch Bay. Previous work of this kind has been limited to the addition of two extra velocity-based terms with application to U-tube data [2]. State-of-the-art system identification techniques are to be used here which allow the addition of force and velocity based terms. The aim was to produce an extended equation giving accurate results with as few extra terms as possible. The extra terms may be inferred from knowledge of the flow phenomena involved or determined purely through sophisticated system identification techniques based on NARMAX routines [3] where the equation structure is obtained automatically and the extra terms may have no obvious relation to the flow phenomena involved.

In both procedures the first stage is to 'fit' the equation structure to the measured data. This gives the mean square error and the relative magnitude of the various terms in the equation, enabling the less significant terms to be removed to give a 'parsimonious' equation. The second stage is to predict the measured force data by solving the resulting equation. In this paper it will be demonstrated that excellent fits are always produced by a simple extension to Morison's equation while predictions are surprisingly little better than the Morison prediction. Improved fits are also obtained by the addition of a single term which is linearly independent of the others enabling an improved force classification into drag, inertia and history to be made. The history term is associated with the effect of vortex shedding.

2 Vortex Shedding and the History Effect

It is well known that the time-history of the wave-force on a cylinder can be due to complicated flow effects which differ from one situation to another. If the Morison equation is to predict accurately, all nonlinear effects must be represented by the nonlinear 'drag' term proportional to $u|u|$. The linear inertia component is in part due to the inviscid effect of flow acceleration. Expansion of the drag term as a polynomial gives

$$u|u| = a_1 u + a_3 u^3 + a_5 u^5 \ldots \tag{2}$$

which shows that even if the flow velocity is a sinusoid $u(t) = U_0 \sin(2\pi t/T)$ the force signal will contain all odd harmonics. One immediately sees that the explanation for the failure of Morison's equation to predict the higher frequency behaviour of the force signal is that the relative size of *all* harmonic components must be fixed by the one coefficient C_d.

It is not possible to link any physical effect to drag and inertia forces in a precise way although it is known that the modification of C_d from zero and C_m from 2 is due to viscous effects. However some broad connections can be made. In a sinusoidal flow starting instantaneously from rest a wake is generated in the first half cycle as the flow separates and vorticity is shed, forming recirculation zones for $KC \geq 2$. (For $KC \leq 2$ detailed description of vorticity behaviour is given in [4].) If KC is large enough these recirculation zones detach themselves, a process known as vortex shedding. The rate at which vorticity is shed at separation is equal to $\pm\frac{1}{2}u_s^2$, where u_s is the velocity just outside the boundary layer at separation. $u|u|$ is thus roughly proportional to the rate of shedding of vorticity and the drag term in Morison's equation may be associated with this effect.

As the flow reverses in the following half cycle, the previously shed vorticity is convected back around the cylinder, a phenomenon sometimes referred to as wake re-encounter. This clearly will affect separation positions, the velocities at separation and thus the part of the force generated by the newly forming wake while the previously shed vorticity generates the remaining part of the total force. Dividing the influence of shed vorticity in this way is justified if one considers the wake to be composed as a series of small 'discrete' vortices, released at the separation positions and moving by inviscid interaction since the influence of each vortex generates a force component given by the Blasius equation, e.g. [5]. The history of the wake behaviour and vortex movement are to some extent accounted for by drag and inertia terms. However, vortex shedding is generally complex, e.g. see [6], and is not well represented in many situations.

Since the drag term is associated with vorticity generation and the history of vortex shedding can be a significant effect, one might expect the additional influence of vortex shedding on force to be modelled by higher order and time derivative terms in F. As a further rationale, it is common practice in system identification to include output terms to model history effects in order to produce a parsimonious model. Initially we thus included additional terms proportional to F^2, F^3, $\dot{F}$ and $\ddot{F}$ which are in fact the terms in the equation for the Duffing oscillator. After some preliminary tests on U-tube data it became apparent that the F^2 term could be discarded as insignificant; the model also showed a degree of improvement when the F^3 term was replaced by one with the form $F|F|$. The form of the extended Morison equation or Morison/Duffing equation is thus

$$\alpha_1\ddot{F} + \alpha_2\dot{F} + F + \alpha_3 F|F| = \frac{1}{2}\rho D C_d u|u| + \frac{1}{4}\pi\rho D^2 C_m \dot{u} \tag{3}$$

The system identification and parameter estimation techniques described in the next section enable the determination of the coefficients α_1, α_2, α_3, C_d and C_m which give the best fit to the measured data. The relative importance of the new terms may also be established. We refer to these extra terms as 'history' terms although the drag and inertia inevitably contain history effects as we have explained. However the additional terms are specifically included to model the 'gross' history effect of vortex shedding.

While one aim is to improve force prediction, another is to improve force classification by improving the fit of the equation to the measured data. With the Morison equation, estimates of C_d and C_m are biased by the residual error which has a structure determined by the flow mechanisms. The history terms should improve the fit and therefore give improved estimates of the contribution from drag, inertia and history. If all the new terms are included in the model, the high degree of correlation between them can produce a condition of near linear dependence, and in this case the weighting between terms can be somewhat arbitrary. If the fit is improved by a smaller model which does not show linear dependence between terms then an improved classification into drag, inertia and history is thought to be justified. Terms which are not linearly dependent can of course still be *correlated* however they will have a unique harmonic structure, i.e. they have a clear identity.

3 System Identification and Parameter Estimation.

The first of the two main problems in identifying a mathematical model of an input-output system is that of structure detection, i.e. what is the form of the equation of the underlying process? In this study the problem is bypassed by adopting the form (3) on heuristic grounds.

Having obtained a model structure the next problem is that of parameter estimation, i.e. how to determine C_d, C_m and $\alpha_1 \ldots \alpha_3$ in equation (3). This is accomplished by minimising the difference between the model output and the measured output data which correspond to the measured input. Suppose N sampled records of force, velocity and acceleration are available i.e. $\{F_i, u_i, \dot{u}_i : i = 1, \ldots, N\}$ where F_i is the i^{th} sampled force value etc. At each sampling instant (by hypothesis) the data satifies the equation

$$\alpha_1\ddot{F}_i + \alpha_2\dot{F}_i + F_i + \alpha_3 F_i|F_i| = \beta_1 u_i|u_i| + \beta_2\dot{u}_i + \zeta_i \tag{4}$$

where β_1 and β_2 are introduced as a convenient shorthand for the constants in equation (3). $\alpha_1, \ldots, \alpha_3, \beta_1$ and β_2 are *estimates* of the parameters here and ζ_i represents the error or residual in the model at instant i. The least-squares estimates of the parameters are formed by minimising the sum of the squared errors

$$J = \sum_{i=1}^{N} \zeta_i^2 \tag{5}$$

with respect to variations of the parameter estimates. The problem is best expressed in matrices. Assembling all equations (3) for $i = 1, \ldots, N$ gives

$$\begin{vmatrix} F_1 \\ F_2 \\ \vdots \\ F_i \\ \vdots \\ F_N \end{vmatrix} = \begin{vmatrix} \ddot{F}_1 & \dot{F}_1 & F_1|F_1| & u_1|u_1| & \dot{u}_1 \\ \ddot{F}_2 & \dot{F}_2 & F_2|F_2| & u_2|u_2| & \dot{u}_2 \\ \vdots & \vdots & \vdots & \vdots & \vdots \\ \ddot{F}_i & \dot{F}_i & F_i|F_i| & u_i|u_i| & \dot{u}_i \\ \vdots & \vdots & \vdots & \vdots & \vdots \\ \ddot{F}_N & \dot{F}_N & F_N|F_N| & u_N|u_N| & \dot{u}_N \end{vmatrix} \begin{vmatrix} \alpha_1 \\ \alpha_2 \\ \alpha_3 \\ \\ \beta_1 \\ \beta_2 \end{vmatrix} + \begin{vmatrix} \zeta_1 \\ \zeta_2 \\ \vdots \\ \zeta_i \\ \vdots \\ \zeta_N \end{vmatrix} \tag{6}$$

or

$$\{F\} = [A]\{\beta\} + \{\zeta\} \tag{7}$$

in matrix notation (square brackets denote matrices, curved brackets denote vectors), $[A]$ is called the design matrix, $\{\beta\}$ is the vector of parameters and $\{\zeta\}$ is the vector of residuals. In this notation the sum of squared errors (5) is

$$\{\zeta\}^T\{\zeta\} = (\{F\}^T - \{\beta\}^T[A]^T)(\{F\} - [A]\{\beta\}) \tag{8}$$

Minimising this expression with respect to the parameter estimates yields the well-known normal equations for the least-squares estimates.

$$[A]^T[A]\{\beta\} = [A]^T\{F\} \tag{9}$$

which are trivially solved by

$$\{\beta\} = ([A]^T[A])^{-1}[A]^T\{F\} \tag{10}$$

provided that $[A]^T[A]$ is invertible. Because of random errors in the measurements, different samples of data will contain different noise components, consequently they will lead to slightly different parameter estimates. The parameter estimates therefore constitute a random sample from a population of possible estimates; this population being characterised by a probability distribution. Clearly, it is desirable that the expected value of this distribution should coincide with the true parameters. If such a condition holds, the parameter estimator is said to be *unbiased.* Now, given that the unbiased estimates are distributed about the true parameters, knowledge of the variance of the parameter distribution would provide valuable information about the possible scatter in the estimates. In fact, this information is readily available; the covariance matrix for the parameters is defined as

$$[C](\hat{\beta}) = E[(\{\hat{\beta}\} - E\{\hat{\beta}\}).(\{\hat{\beta}\} - E\{\hat{\beta}\})^T] \tag{11}$$

where the carets are used to emphasize the fact that quantities are estimates and the expectation E is taken over all possible estimates. The diagonal elements C_{ii} are the variances of the parameter estimates $\hat{\beta}_i$. Under a number of mild assumptions it is possible to show that, given an estimate $\{\hat{\beta}\}$

$$[C] = \sigma_\zeta^2.([A]^T[A])^{-1} \tag{12}$$

where σ_ζ^2 is the variance of the residul sequence ζ_i obtained by using $\{\hat{\beta}\}$ to predict the output. The standard deviation for each parameter is therefore:

$$\sigma_i = \sigma_\zeta\sqrt{([A]^T[A])^{-1}_{ii}} \tag{13}$$

If the parameter distributions are Gaussian, standard theory yields a 95% confidence interval of $\{\hat{\beta}\} \pm 1.96\{\sigma\}$, i.e. there is a 95% probability that the true parameters fall within this interval.

In order to determine whether a term is an important part of the model, a significance factor can be defined as follows. Each model term $\theta(t)$, e.g. $\theta(t) = F(t)$ or $\theta(t) = F(t)|F(t)|$, can be used on its own to generate a time-series which will have variance σ_θ^2. The significance factor s_θ is then defined by

$$s_\theta = 100\frac{\sigma_\theta^2}{\sigma_F^2} \tag{14}$$

where σ_F^2 is the variance of the estimated force, i.e. the sum of all the model terms. Roughly speaking, s_θ is the percentage contributed to the model variance by the term θ.

Having obtained a set of model parameters, it is necessary to check the accuracy of the model. The simplest means of doing this is to plot and compare the measured force F_i with the curve-fit value

$$\hat{F}_i = -\alpha_1\ddot{F}_i - \alpha_2\dot{F}_i - \alpha_3 F_i|F_i| + \beta_1 u_i|u_i| + \beta_2\dot{u}_i \tag{15}$$

based on the estimated parameters. One can also use a numerical measure of the closeness of fit; the measure adopted here is the normalised mean-square error or MSE defined by

$$MSE(\hat{F}) = \frac{100}{N\sigma_F^2}\sum_{i=1}^{N}(F_i - \hat{F}_i)^2 \tag{16}$$

This MSE has the following useful property; if the mean of the force signal $\overline{F}$ is used as the model i.e. $\hat{F}_i = \overline{F}$ for all i, the MSE is 100%, i.e.

$$MSE(\hat{F}) = \frac{100}{N\sigma_F^2}\sum_{i=1}^{N}(F_i - \overline{F})^2 = \frac{100}{\sigma_F^2}.\sigma_F^2 = 100 \tag{17}$$

A more stringent test of the model validity is to predict the wave force from equation (4) using measured velocities and accelerations only, via some time-stepping procedure. This can then be compared with the measured force.

The most comprehensive set of model validity tests are those of Billings [7]. Briefly, the validity of the model is contingent on the vanishing of certain correlation functions between the input (in this case velocity), and residual data.

4 Application of the New Model Structure.

The measured data may be divided into two broad categories associated with unidirectional onset flows and directional sea-states.

4.1 Unidirectional Onset Flows

The data has been obtained from three sources. Forces on a cylinder in the sinusoidal flow of a U-tube have been measured by Obasaju et. al. [6]. Measurements were made at different values of KC at a given β value and two types of force time-histories were distinguished. For a given situation (defined by KC and β) different

force histories were associated with different modes of vortex shedding and the force history associated with each mode was obtained. The differences could however be quite subtle and force histories were also obtained by averaging over all cycles (and hence all modes) and it is these which we use here. The data were obtained by digitising plots of force against time for KC = 3.31,6.48,11.88,17.5 and 34.68 available with $\beta = 417$.

Forces have also been measured on a cylinder oscillating in still water and a uniform current by Obasaju et.al. [8]. For the latter there is now an additional parameter defining the flow, the ratio of current velocity to the amplitude of the oscillatory velocity, a. Again the data were obtained by digitising plots of force against time, only available for a range of β values. In the situations with a current a single drag term in the Morison equation is maintained, i.e. an 'oscillatory' drag and 'current' drag are not considered separately.

Forces due to random waves have been measured in the Delta flume of the De Voorst facility of Delft Hydraulics. The particular data considered here comes from run OA1F1 which used a smooth fixed vertical cylinder. The waves were generated to give a JONSWAP surface elevation spectrum. The forces were measured on force sleeves placed at three levels on the cylinder. Data from the highest sleeve which always remains immersed is used to give the force with the greatest drag component. The velocity signal was obtained from electromagnetic flowmeters placed adjacent to the cylinder at the same distance from the wave maker. More details of the experiment can be found in [9] and [10] which also contain wave-by-wave Morison analyses of the De Voorst data sets. We plotted the entire velocity, in-line force and transverse force records and analysed the part of the record around the instant when the transverse force was a maximum. This is because the magnitude of the transverse force is thought to be an indicator of the significance of vortex shedding and nonlinearity of the in-line force. 1000 points of the time-history were used for the parameter estimation. The Keulegan-Carpenter number is defined in this case as $\sqrt{2}u_{rms}T_p/D$ where u_{rms} is the rms value of the horizontal velocity and T_p is the period associated with the peak in the velocity spectrum. For the data analysed KC was found to be 5.03 and β to be approximately 4 x 10^4.

First Morison's equation was fitted to each data set and the resulting drag and inertia coefficients are given together with the curve fit MSEin Table 1. The percentages of mean square drag and inertia are also given, normalised by the mean square force. As expected the drag proportion increases and the inertia proportion decreases, as KC increases. The MSE can be quite large, particularly with KC between 10 and 14 without and with a current. In all the following tables, the inertia coefficients for the oscillating cylinder data have been incremented by 1 in order to include a Froude-Krylov component. This was done in order to facilitate comparison with the U-tube data. However, it seemed hardly worthwhile to increment the raw data and for this reason the inertia component is smaller for the oscillating cylinder data than it would be for a fixed cylinder in kinematically equivalent oscillatory flow. Force histories with KC equal to 11.88, 17.5 and 34.68 are shown in Figures 1, 2 and 3 with the Morison fits. Figure 4 shows the Morison fit to the De Voorst data which is very close as would be expected with such a small nonlinear component.

Fits using the Morison/Duffing equation (3) were originally made by using a five point centred difference formula to estimate the derivatives $\dot{F}$ and $\ddot{F}$ and this showed considerable improvements over the Morison fit. However, the estimated derivatives were noisy. The influence of the noise was reduced by adopting the discrete or NARMAX version of equation (3) given by

$$F_i = a_1 F_{i-1} + a_2 F_{i-2} + a_3 F_{i-1}|F_{i-1}| + b_1 u_{i-1} + b_2 u_{i-2} + b_3 u_{i-1}|u_{i-1}| \qquad (18)$$

The results of fitting this equation to the data are given in Table 2 and the MSE values are now seen to be very low. Curve-fits corresponding to Figures 1, 2 and 3 are given in Figures 5, 6 and 7 and are almost within plotting accuracy. This is also the case for the De Voorst data but this is not shown since the Morison fit was also very close. The history percentages in Table 2 are due to the sum of all the extra terms involving F. In this case the percentages of drag, inertia and history are not meaningful due to linear dependencies between the terms. Predicted force output may be obtained from equation (18) by stepping F_i forward in time using the measured velocities only and using F_1 and F_2 to start the calculation. Using this procedure the MSE values showed no appreciable improvement over those for the Morison fit.(Since the Morison equation contains only velocity and acceleration terms the MSE for the curve fit is identical to that for the predicted output.) This is a surprising result in view of the excellent curve fits and has yet to be properly understood.

The analysis indicated that the $F|F|$ term in equation (18) generally made the most significant contribution to the fit and an equation structure including only this extra term was tested:

$$F + \alpha F|F| = \beta_1 u|u| + \beta_2 \dot{u} \qquad (19)$$

The results are given in Table 3. The MSE's are still significantly below the values for the Morison fits where the MSE was high. In Table 3 the values of α are only meaningful when F is normalised in some way. In this case this was achieved by dividing by $\frac{1}{2}\rho D U_0^2$ for sinusoidal flow and, equivalently, by $\rho D u_{rms}^2$ for the De Voorst data. For this model structure the terms are not linearly dependent and so the percentages of drag, inertia and history can be considered to be meaningful. A practical demonstration of this independence can be seen in the case with $KC = 14$ and $a = 1.01$. Here the Morison fit is excellent and the MSE is virtually unchanged by the addition of the $F|F|$ term. The percentage history is negligible indicating that the drag and inertia components have suffered no interference. This example corresponds to the case of so-called 'pulsatile' flow where the presence of the current ensures that there is no flow reversal; as a consequence the wake is convected away from the cylinder and one would not expect to observe gross history effects. The history effect is most significant for KC between 10 and 14 when the MSE for the Morison fit is large. This range of KC has particularly large lift forces [6] [8] which are caused by vortex shedding, providing quantitative evidence of the link between history and vortex shedding.

The values of the coefficients C_m, C_d and α vary markedly from one situation to another and so we are clearly not providing a universal curve-fit equation. However, it is interesting to note that the sinusoidal case with $KC = 6.48$ and the De Voorst case with $KC = 5.03$ have very similar values for C_m and α with different C_d's, which is the only indication of the difference in β values.

The prediction of the Morison/Duffing equation gave little improvement on the Morison prediction and the predictions from equation (19) are likely to be worse. The exact solution may easily be obtained and shows clear bifurcation characteristics as $u(t)$ changes. Specifically, at one sampling instant the equation can have three real roots and only one at the next instant. This effect is shown in Figure 8 where the

predicted force history for $KC = 11.88$ is shown. Although the bifurcation does not occur in every situation equation (19) is clearly of no value as a predictor.

4.2 Directional Sea State.

The above data is valuable in that it is of high quality and enables new model structures of the force equation with vortex shedding to be investigated. The flow situations are however idealised with Reynolds numbers well below full scale values. The Reynolds number for the De Voorst data is closer to full scale but the KC value is low giving inertia-dominated forces which are inevitably fitted well by Morison's equation.

In this section the new model structures are fitted to forces and velocities measured on the Christchurch Bay Tower described in [11]. The same cylinder was used in the De Voorst tests but the sea states have greater wave heights (up to 7m against 2m at De Voorst) and are directional with a prominent current. The velocities were measured with calibrated perforated ball meters attached at a distance of 1.228m from the cylinder axis. This will not give the exact velocity at the centre of the force sleeve unless waves are unidirectional with crests parallel to the line joining the velocity meter to the cylinder. This is called the Y direction and the normal to this, the X direction. The waves are however always varying in direction so data was chosen here from an interval when the oscillatory velocity in the X direction was large and that in the Y direction small. A sample of 1000 points fitting these criteria is shown in Figure 9. It can be seen that the current is mainly in the Y direction. In this case the velocity ball is upstream of the cylinder and interference by the wake on the ball will be as small as possible with this arrangement. Clearly the data is not of the same quality as that section 4.1 but it should be sufficiently reliable to test the model equation structures.

The acceleration values corresponding to the velocities in Figure 9 are shown in Figure 10. In the Y direction the magnitudes are small with a relatively high frequency content. The KC values in the X and Y directions are 19.7 and 4.85 respectively. The ratios of current velocity to $\sqrt{2}u_{rms}$, a, are 0.16 and 2.1 in the corresponding directions. To obtain α in equation (19) the forces in the X and Y direction were normalised by $\rho D u_{rms}^2$ where u_{rms} is in the corresponding direction. The results of the fits are given in Table 4 for forces and velocities in the X and Y directions and also for forces resolved in the instantaneous velocity direction and perpendicular to it, which are strictly the in-line and out-of-line forces. The magnitude of velocity is shown in Figure 11 with the angle of the velocity vector relative to the X direction. This angle shows considerable variation and Figure 12 shows that the normal acceleration can be greater than the in-line acceleration.

The MSE of the Morison fit to the X force is high; the time histories are given in Figure 13. The peaks in force are considerably underestimated and the high frequency components of force are largely omitted. The fit including the $F|F|$ term shows considerable improvement and the curves are shown in Figure 14. The force peaks are now slightly overpredicted and the harmonic content is better represented. The Morison/Duffing equation gives a remarkably accurate fit with the MSE reduced by a factor of over a 100 over the Morison fit. However prediction by this equation is slightly worse than the Morison equation as it was for the unidirectional flows. The results for the Y direction are even more spectacular. The MSE for the Morison fit is now 100% indicating a total lack of correlation between the Morison equation and the measured data. The time histories are shown in Figure 15. The inclusion of

the $\alpha F|F|$ term reduces the MSE by a factor of 3 and the time histories are shown in Figure 16. Remarkably the Morison/Duffing equation again reduces the MSE by a factor of 100 over the Morison fit; the time histories are shown in Figure 17. In this case the drag and inertia components are negligible and history dominates as would be expected. In the X direction, drag and history components are of similar magnitude and are greater than the inertia component. The importance of history in both directions implies that vortex shedding is a prominent influence.

Results with forces resolved in the instantaneous velocity direction are similar to those in the X direction although the value for a has changed from 0.16 to 1.7. However the force normal to the instantaneous velocity direction is also substantial as shown in Figure 18. The fit of the Morison equation is shown in Figure 19, giving a MSE of 70% with no drag and 30% inertia. The addition of the $\alpha F|F|$ again significantly improves the fit as shown in Figure 20, although the peak forces are substantially overestimated. The Morison/Duffing equation, based on equation (18), obviously cannot be applied since the velocity is always zero. Overall there would appear to be no advantage in resolving forces parallel and normal to the instantaneous velocity.

5 Discussion

New model structures including additional force rather than velocity terms have proved very effective in fitting measured force and velocity data from various sources. These new equations were first tested with U-tube data for a constant β value where the occurrence of vortex shedding as a function of KC is known through the magnitude of the lift force [6] [8]. When the lift is small, at low KC, the Morison fit is good, and when it is high, of similar magnitude to the in-line force, the Morison fit may be poor. It should be noted that the Morison fit can be quite good when lift is significant, e.g. with $KC = 17.5$, presumably due to the way in which the vortex shedding organises itself. The curve fits by the Morison/Duffing equation were always accurate to almost plotting accuracy with $\alpha F|F|$ usually the most significant term. The addition of this term alone to Morison's equation significantly improves the quality of the curve fit particularly when the Morison fit is poor. Since the term is linearly independent of the other terms the force may be classified as drag, inertia and history (although it is known the drag and inertia inevitably contain some history effects). In this way the link between error in the Morison equation, history and vortex shedding is quantified through data analysis. Corresponding effects were found when a current was superimposed on sinusoidal oscillation. The random wave data from the De Voorst flume unfortunately adds little to the discussion since the force was inertia-dominated.

A disappointing aspect of this study is the poor force prediction by the Morison/Duffing equation which is far from well understood. However when the NARMAX procedures are allowed to choose terms automatically using a structure detection algorithm [3], the fits and predictions were both very close to the measured data. Unfortunately, the terms chosen were often of an intangible form and had little consistency from one situation to another. New work is in progress to optimise the form of the underlying differential equation structure and this could produce more consistent results.

With the addition of the $\alpha F|F|$ term the C_d and C_m coefficients showed less variation with KC (for a fixed β) than for the Morison equation alone although they were far from constant. The two positive results are thus the excellent curve fits

obtained by the Morison/Duffing equation with only three (four in the discrete case) extra terms, and the improved force classification into drag, inertia and history (using only one extra term).

These procedures worked correspondingly well on wave force and velocity data obtained from the Christchurch Bay Tower. These data were not so reliable as those measured in idealised situations but they gave at least a qualitative assessment of the procedures. A suitable sample was chosen for analysis and turned out to give a very severe test. The Morison fit was poor with the force peaks grossly underestimated. The history term gave a similar contribution to the drag in one direction (and about twice that of the inertia term) and was dominant in the other direction. On the basis of analysis in unidirectional flows, this indicates that the poor performance of Morison's equation is due to vortex shedding, a result that was not known *a priori*. The converse of the argument is that if a poor fit by the Morison equation is not associated with a significant history term then this is due to something other than vortex shedding.

The value of this analysis lies particularly with directional waves where the lift force due to vortex shedding may not be isolated. It is demonstrated here that resolving in the instantaneous velocity direction leaves a significant acceleration in the normal direction generating a 'lift' inertia force. Resolving in this way is considered to be of little value.

When considering the poor fit by the Morison equation to this sample of data, it should be remembered that it was obtained from a coastal situation, where wave characteristics are known to be rather different from those offshore where, for example, waves and currents are more likely to be in the same direction. It is the intention to analyse data from more sources, from measurements in a wave basin, on a cylinder oscillating in a prescribed manner and, if possible, from further measurements at sea. In this way a realistic assessment of the importance of vortex shedding on wave forces on offshore structures will be obtained.

6 Conclusions.

1. An extension to the Morison equation including terms in $F|F|$, $\dot{F}$ and $\ddot{F}$ gives excellent curve fits to all the wave force data analysed for this paper. The inclusion of extra terms in the force rather than velocity is argued from consideration of vorticity behaviour. The errors in force prediction however are only similar to those given by the Morison equation.
2. Significantly improved fits are also obtained by including the $F|F|$ term alone, particularly when the Morison fit is poor. Since this term is linearly independent of the others, an improved force classification in drag, inertia and history is proposed. In unidirectional flow the association of the history term with vortex shedding is confirmed by the occurrence of lift.
3. In a directional sea state at the Christchurch Bay Tower the Morison fit is poor. There is significant improvement with the $F|F|$ term with a correspondingly prominent history component indicating the significance of vortex shedding.
4. In directional seas, where lift due to vortex shedding cannot be isolated, it is suggested that the data analysis described here is a useful tool for diagnosing the significance of vortex shedding. It should be stressed however that an improved fit using the $F|F|$ term is not absolute proof of vortex shedding, it is simply consistent with observations in unidirectional flow.

Acknowledgements.

Thanks are due to Delft Hydraulics for access to the wave force data obtained in the Delta flume in their De Voorst facility. This data was provided with the assistance of Malcolm Birkenshaw of the Department of Energy and Professor Peter Bearman and Martin Davies of Imperial college. In particular, the help provided by Martin Davies in translating data into a useful format is much appreciated. Thanks are also due to Dr. Emmanuel Obasaju for making available unpublished data from his experimental work undertaken as a research associate at Imperial College. This project is supported by the Department of Energy through the Marine Technology Directorate's managed programme on the Behaviour of Fixed and Compliant Offshore Structures. This paper will comprise part of the final report to the Department of Energy (to be published by HMSO).

	C_d	C_m	α	Drag %	Inertia %	History %	MSE %
X direction: $a = 0.16, KC = 19.7, \beta = 6e10^4$							
Morison	0.74	1.18	-	55	27	-	19
Morison $+\alpha F\|F\|$	0.42	0.82	0.4	18	13	21	10
Morison/Duffing	0.04	0.03	-	1	0	94	0.2
Y direction: $a = 2.1, KC = 4.85$							
Morison	0.70	0.63	-	6	3	-	100
Morison $+\alpha F\|F\|$	0.39	0.44	0.05	2	1	66	35
Morison/Duffing	0.00	0.00	-	0	0	99	1
'In-line' force: $a = 1.7, KC = 19.8, \beta = 12e10^4$							
Morison	0.65	1.19	-	44	21	-	21
Morison $+\alpha F\|F\|$	0.44	0.84	0.08	20	10	20	11
Morison/Duffing	0.10	0.00	-	1	1	89	0.4
'Out-of-line' force:							
Morison	-	1.05	-	-	30	-	70
Morison $+\alpha F\|F\|$	-	0.41	0.30*	-	5	63	18
* obtained with 'in-line' force normalisation							

Table 4: Model Fits to Sample of Christchurch Bay Data.

KC	β	a	C_d	C_m	Drag %	Inertia %	History %	MSE %
Oscillatory flow data ($KC = \frac{U_0 T}{D}$)								
3.31	417	0.0	-0.26	1.15	0.1	17.7	32.5	0.01
6.48	417	0.0	0.04	1.02	0.01	0.45	84.9	0.007
11.88	417	0.0	0.03	1.01	0.02	0.14	92.6	0.04
17.5	417	0.0	0.15	1.02	0.49	0.21	81.7	0.01
34.68	417	0.0	0.33	1.08	3.62	2.18	48.8	0.10
14.0	929	0.0	0.59	1.01	6.08	1.46	77.7	0.28
18.0	634	0.0	0.54	1.06	6.86	17.13	14.1	1.29
14.0	933	0.18	0.29	1.02	3.15	1.26	55.0	0.62
10.0	1081	0.52	0.54	1.04	12.45	9.45	18.2	2.24
14.0	417	1.01	0.52	1.01	13.1	0.92	29.6	0.09
De Voorst ($KC = \frac{\sqrt{2} u_{rms} T}{D}$)								
5.03	$\approx 4.10^4$	0.0	0.24	0.32	0.54	11.6	44.7	0.79

Table 2: Duffing-Morison Fit to Data.

KC	β	a	C_d	C_m	α	Drag %	Inertia %	History %	MSE %
Oscillatory flow data ($KC = \frac{U_0 T}{D}$)									
3.31	417	0.0	1.09	2.18	0.01	1.8	89.6	0.2	0.17
6.48	417	0.0	1.42	1.59	0.07	12.4	49.8	4.6	0.18
11.88	417	0.0	1.25	0.64	0.22	20.5	5.1	26.7	2.2
17.5	417	0.0	1.85	0.99	0.06	69.7	8.6	1.3	0.59
34.68	417	0.0	1.40	1.12	0.12	63.5	4.6	3.2	0.75
14.0	929	0.0	1.23	0.79	0.21	25.6	0.5	25.7	1.7
18.0	634	0.0	1.45	1.32	0.17	46.9	0.9	9.3	2.3
14.0	933	0.18	0.93	1.18	0.57	30.0	0.7	18.3	2.2
10.0	1081	0.52	0.65	1.20	1.46	18.0	1.0	27.5	1.6
14.0	417	1.01	1.12	1.62	0.44	61.0	2.0	0.5	0.36
De Voorst ($KC = \frac{\sqrt{2} u_{rms} T}{D}$)									
5.03	$\approx 4.10^4$	0.0	0.46	1.55	0.07	1.87	67.0	2.8	2.0

Table 3: Morison $+\alpha F|F|$ Fit to Data.

	C_d	C_m	α	Drag %	Inertia %	History %	MSE %
X direction: $a = 0.16, KC = 19.7, \beta = 6e10^4$							
Morison	0.74	1.18	-	55	27	-	19
Morison $+\alpha F\|F\|$	0.42	0.82	0.4	18	13	21	10
Morison/Duffing	0.04	0.03	-	1	0	94	0.2
Y direction: $a = 2.1, KC = 4.85$							
Morison	0.70	0.63	-	6	3	-	100
Morison $+\alpha F\|F\|$	0.39	0.44	0.05	2	1	66	35
Morison/Duffing	0.00	0.00	-	0	0	99	1
'In-line' force: $a = 1.7, KC = 19.8, \beta = 12e10^4$							
Morison	0.65	1.19	-	44	21	-	21
Morison $+\alpha F\|F\|$	0.44	0.84	0.08	20	10	20	11
Morison/Duffing	0.10	0.00	-	1	1	89	0.4
'Out-of-line' force:							
Morison	-	1.05	-	-	30	-	70
Morison $+\alpha F\|F\|$	-	0.41	0.30*	-	5	63	18
* obtained with 'in-line' force normalisation							

Table 4: Model Fits to Sample of Christchurch Bay Data.

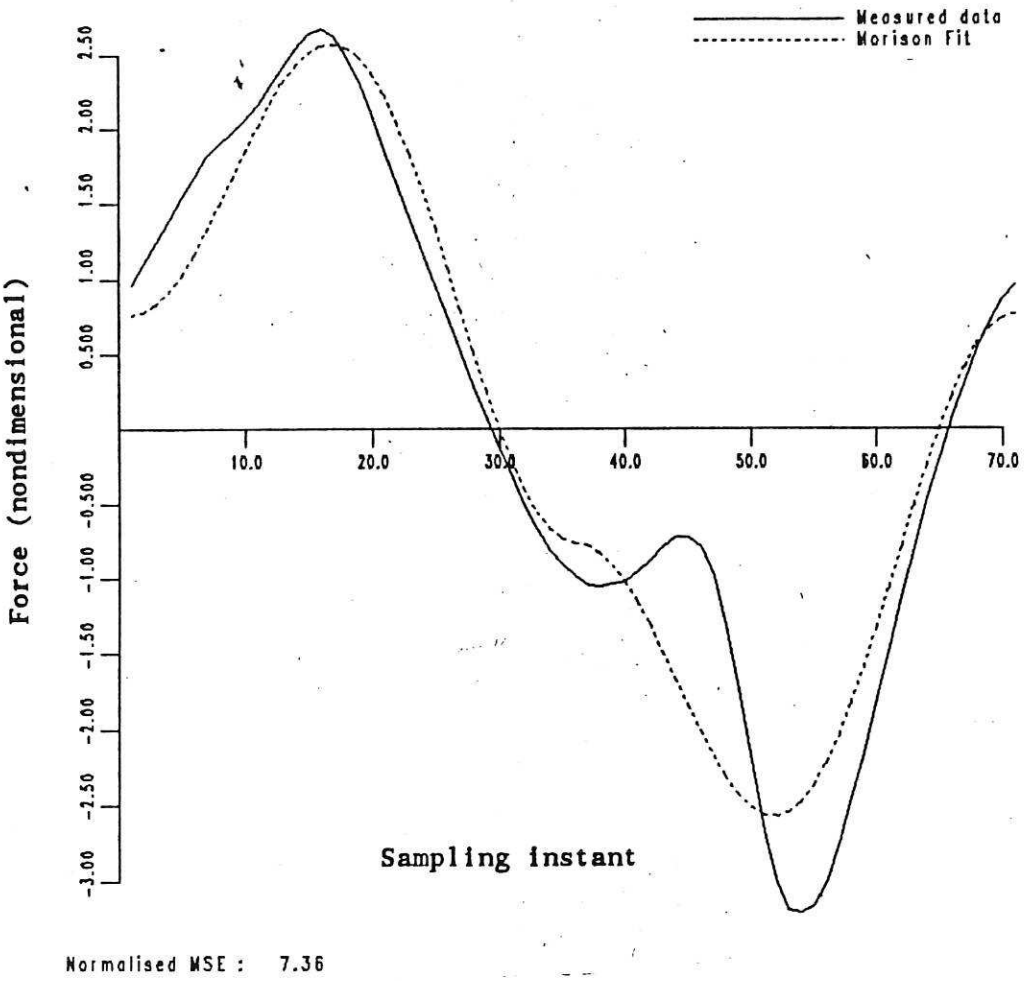

Figure 1. Comparison between measured U-tube data and Morison equation prediction. KC = 11.88.

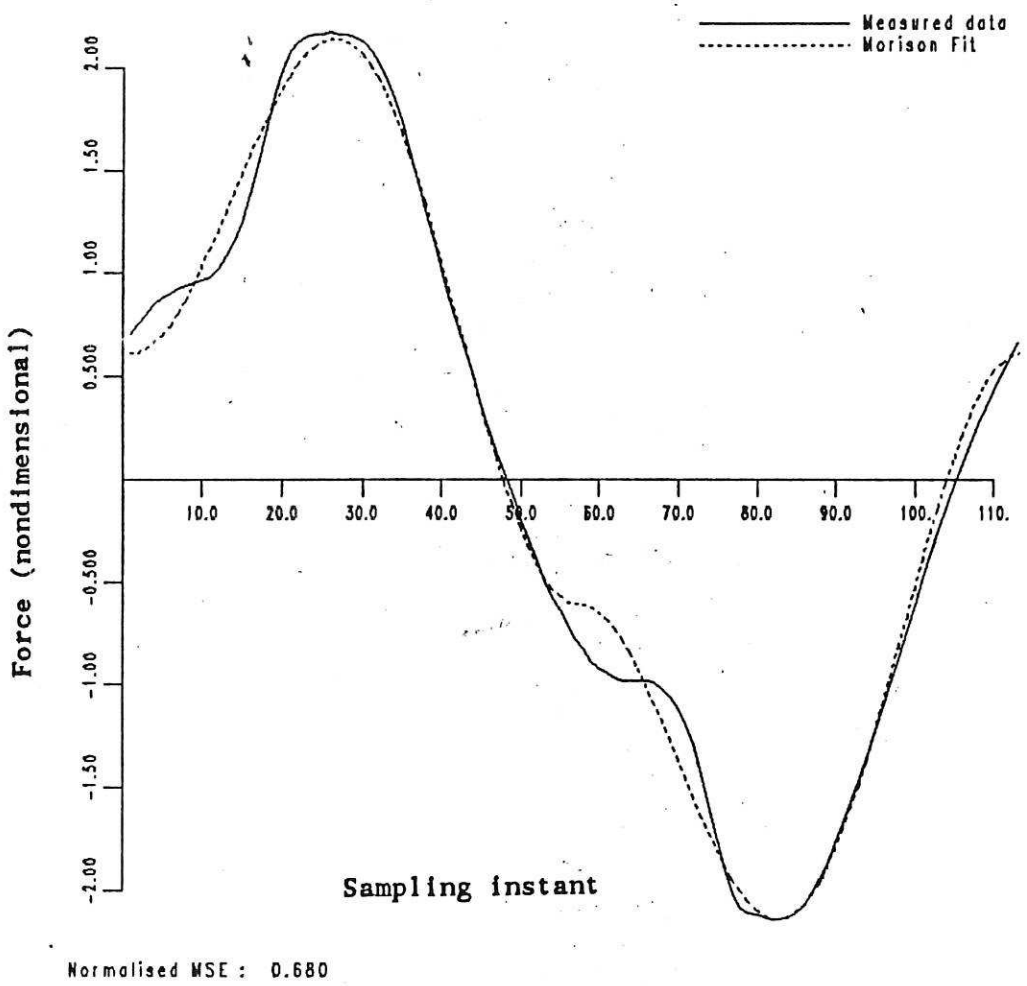

Figure 2. Comparison between measured U-tube data and Morison equation prediction. KC = 17.5.

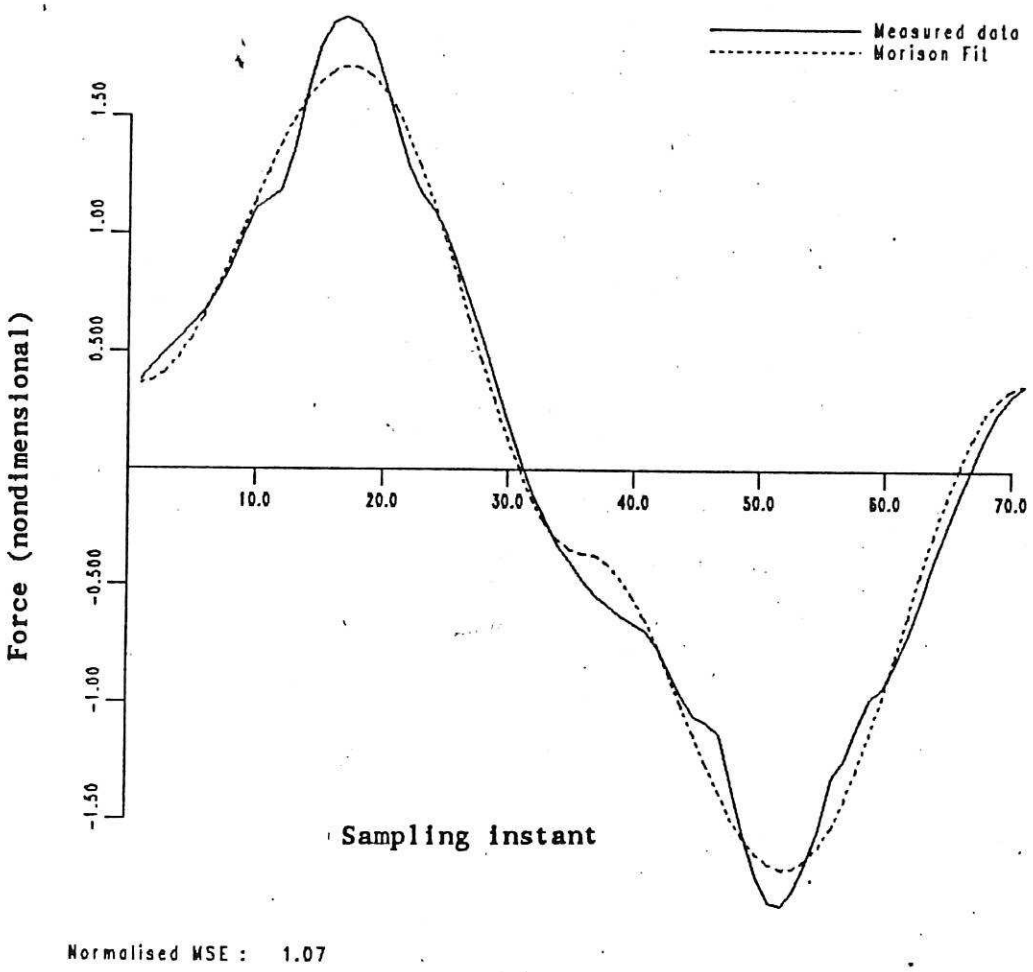

Figure 3. Comparison between measured U-tube data and Morison equation prediction. KC = 34.68.

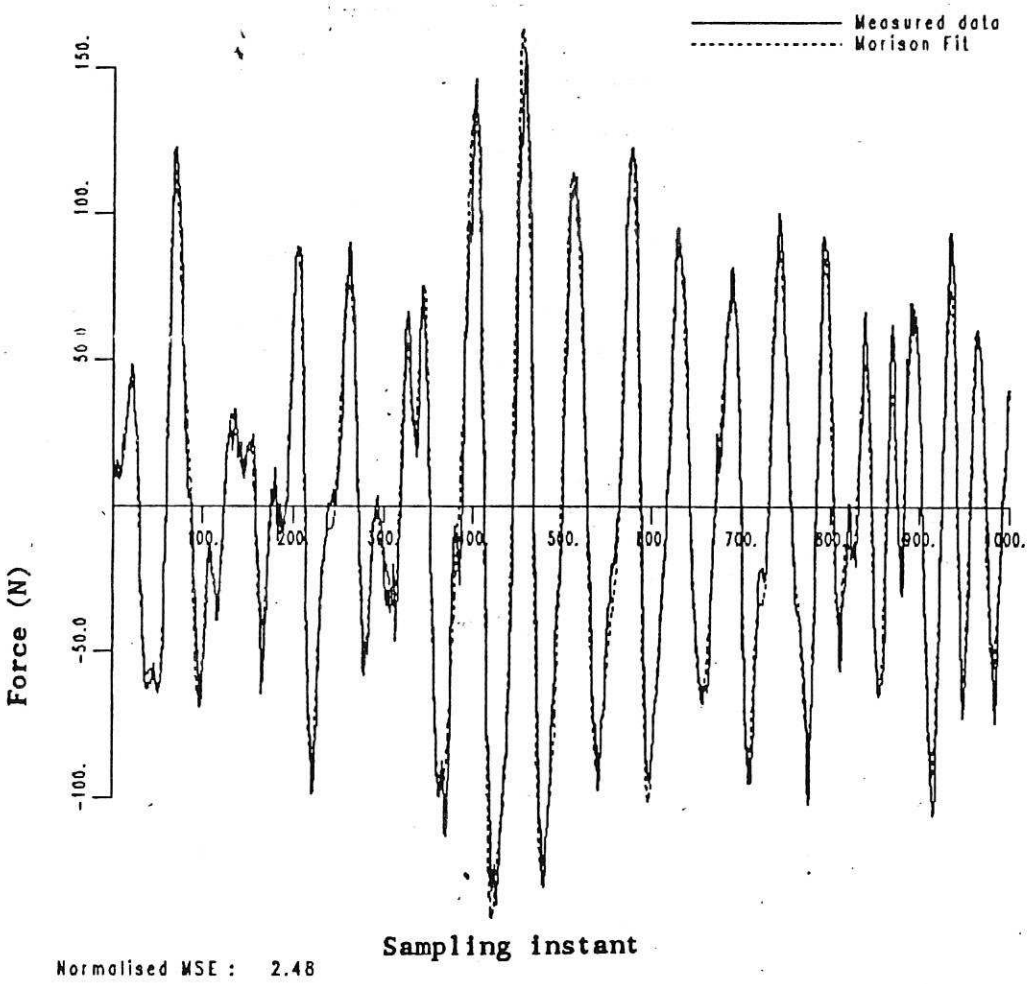

Figure 4. Comparison between a sample of De Voorst force data and the Morison prediction.

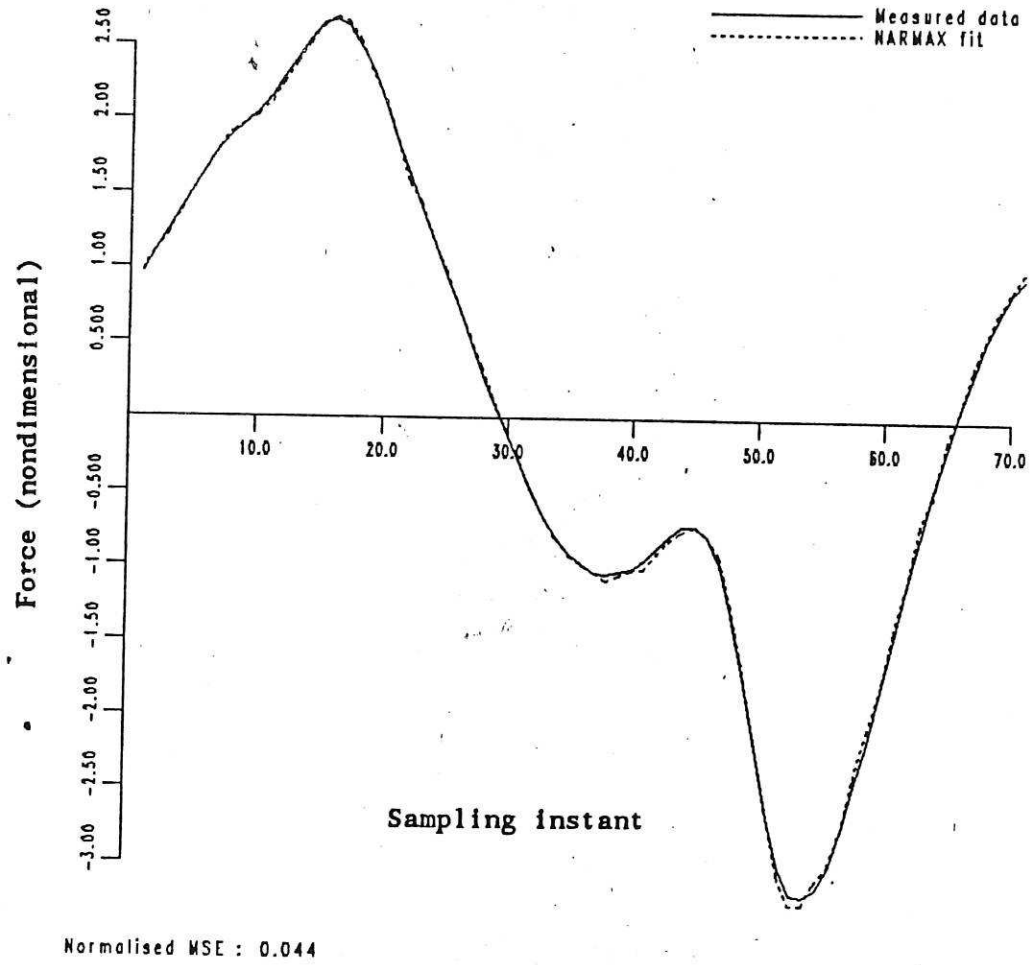

Figure 5. Comparison between measured data and least-squares curve-fit for the Duffing/Morison equation. KC = 11.88.

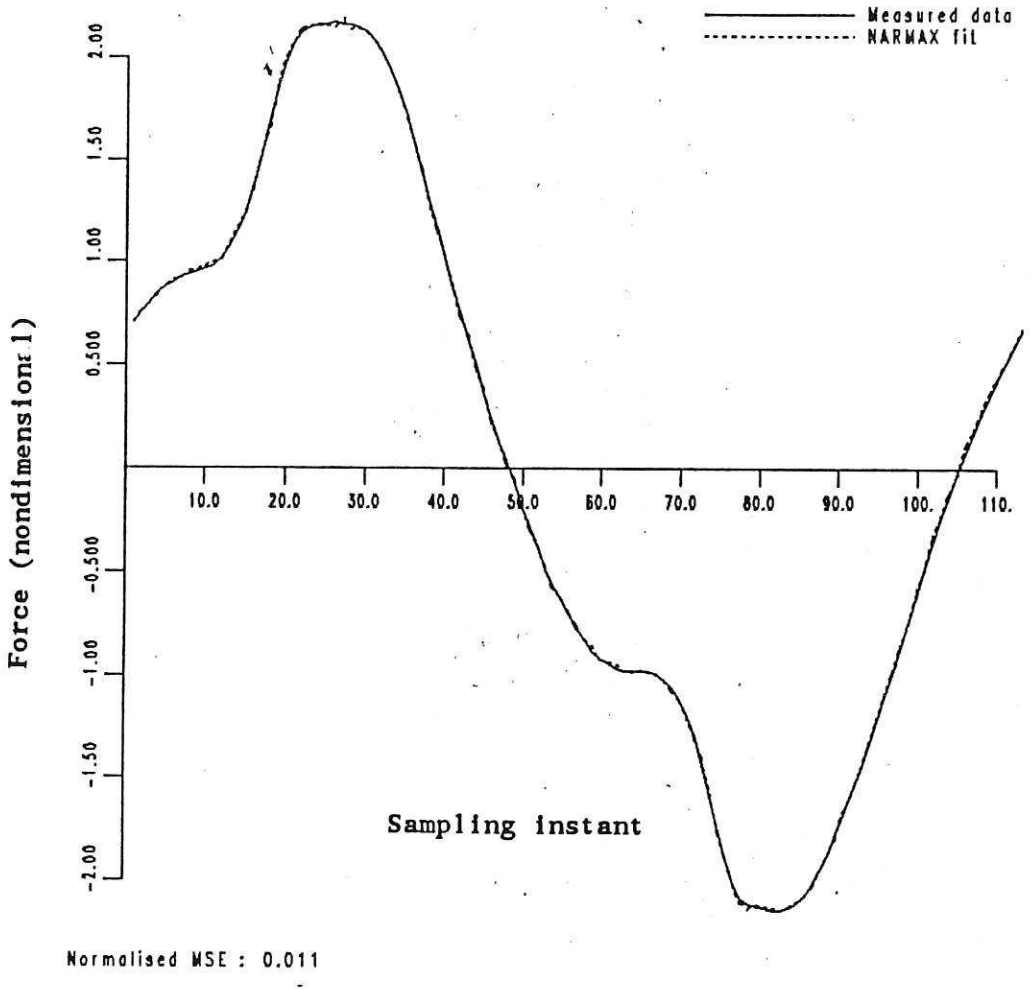

Figure 6. Comparison between measured data and least-squares curve-fit for the Duffing/Morison equation. KC = 17.5.

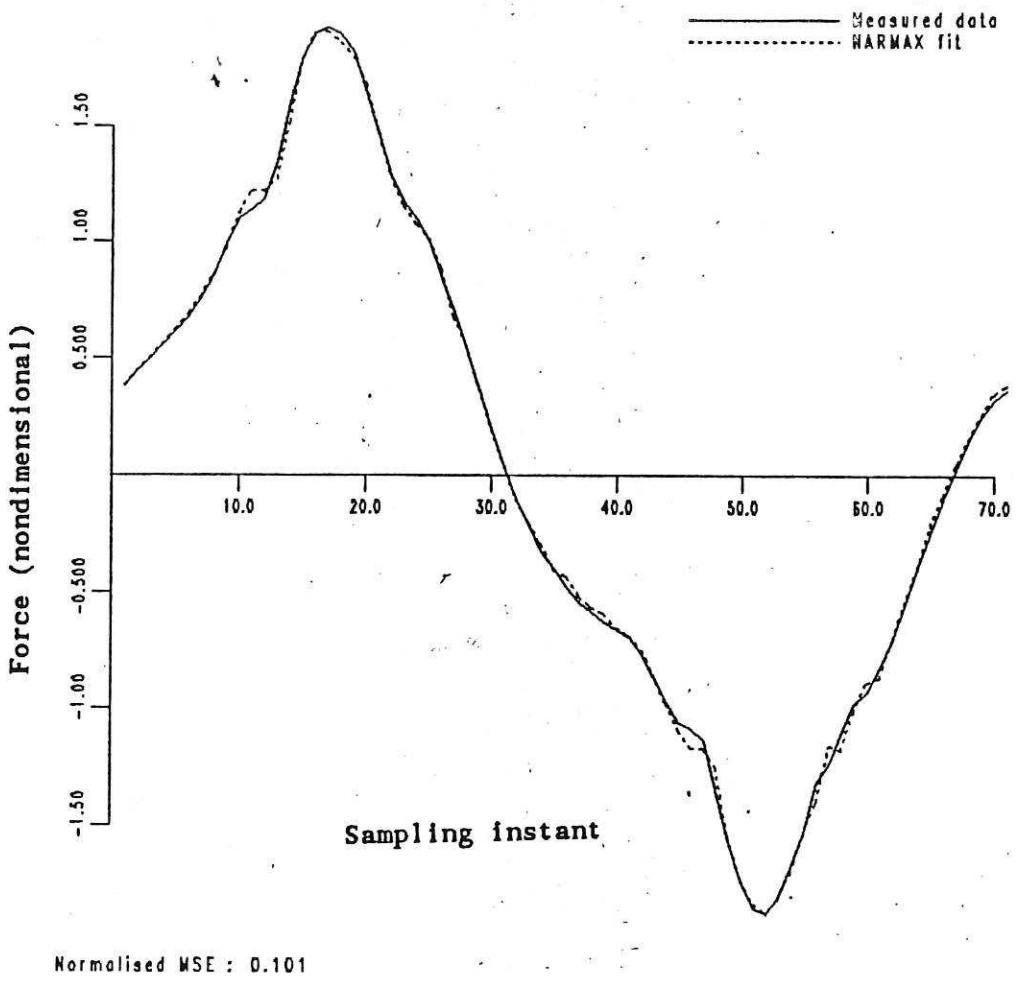

Figure 7. Comparison between measured data and least-squares curve-fit for the Duffing/Morison equation. KC = 34.68.

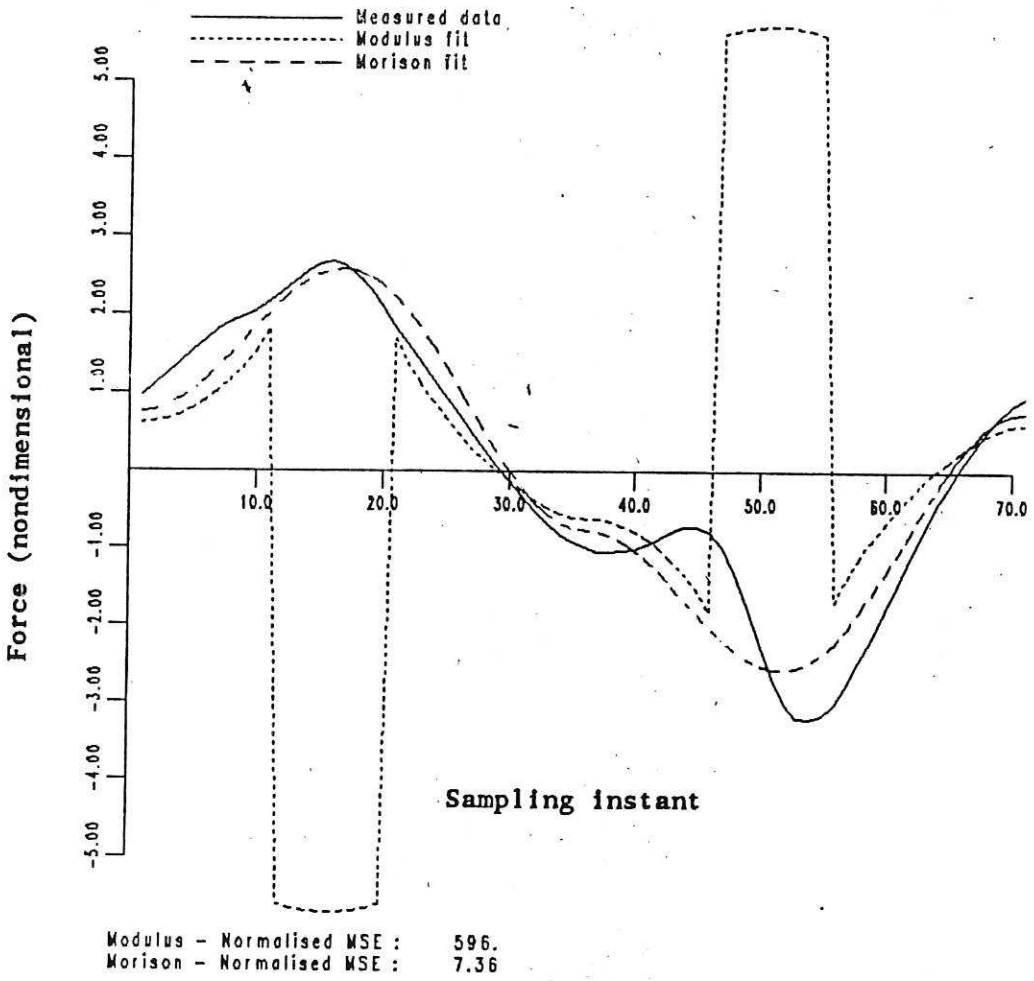

Figure 8. Comparison between measured data and prediction using the Morison + $\alpha F|F|$ model. KC = 11.88.

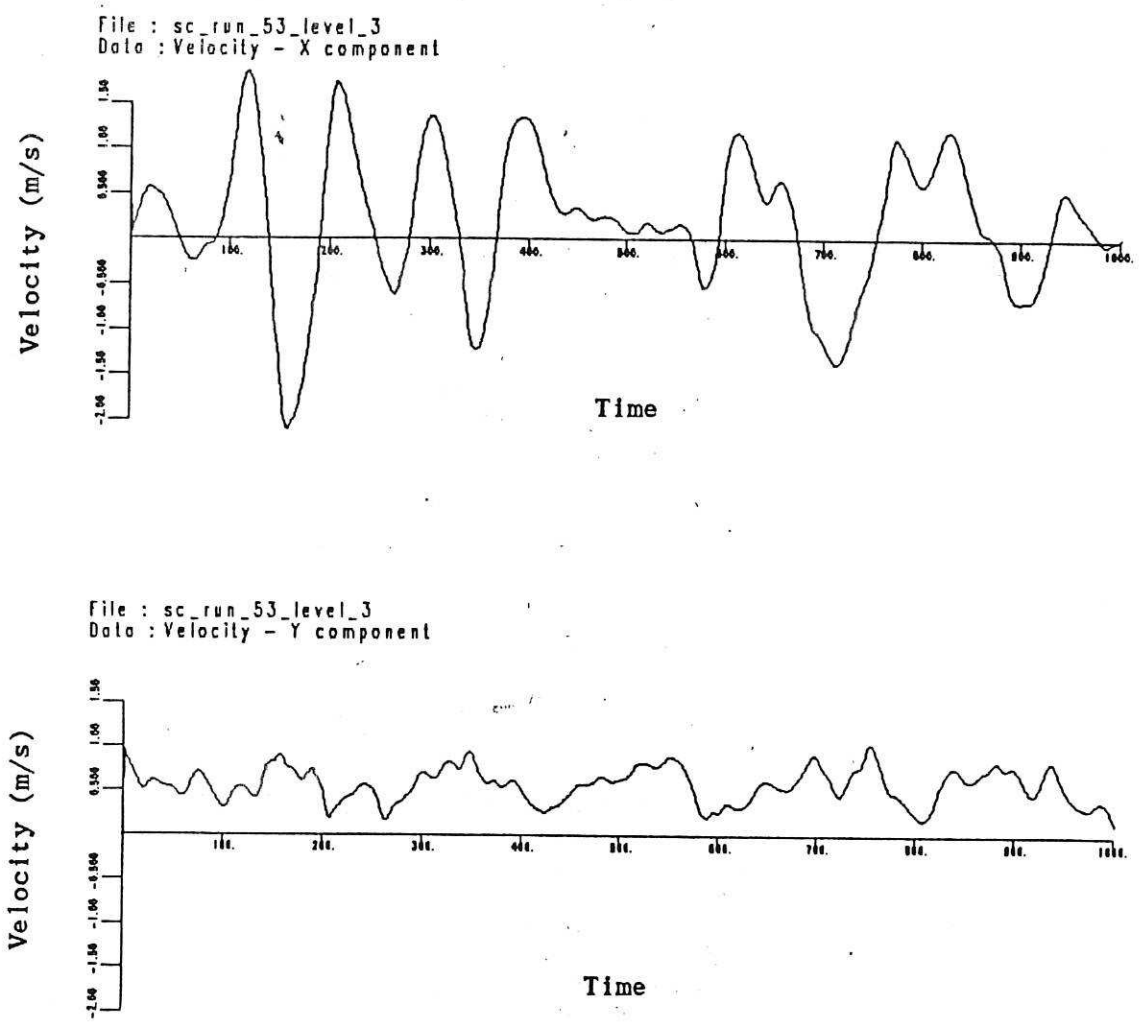

Figure 9. Velocity components in X and Y directions for sample of Christchurch Bay data.

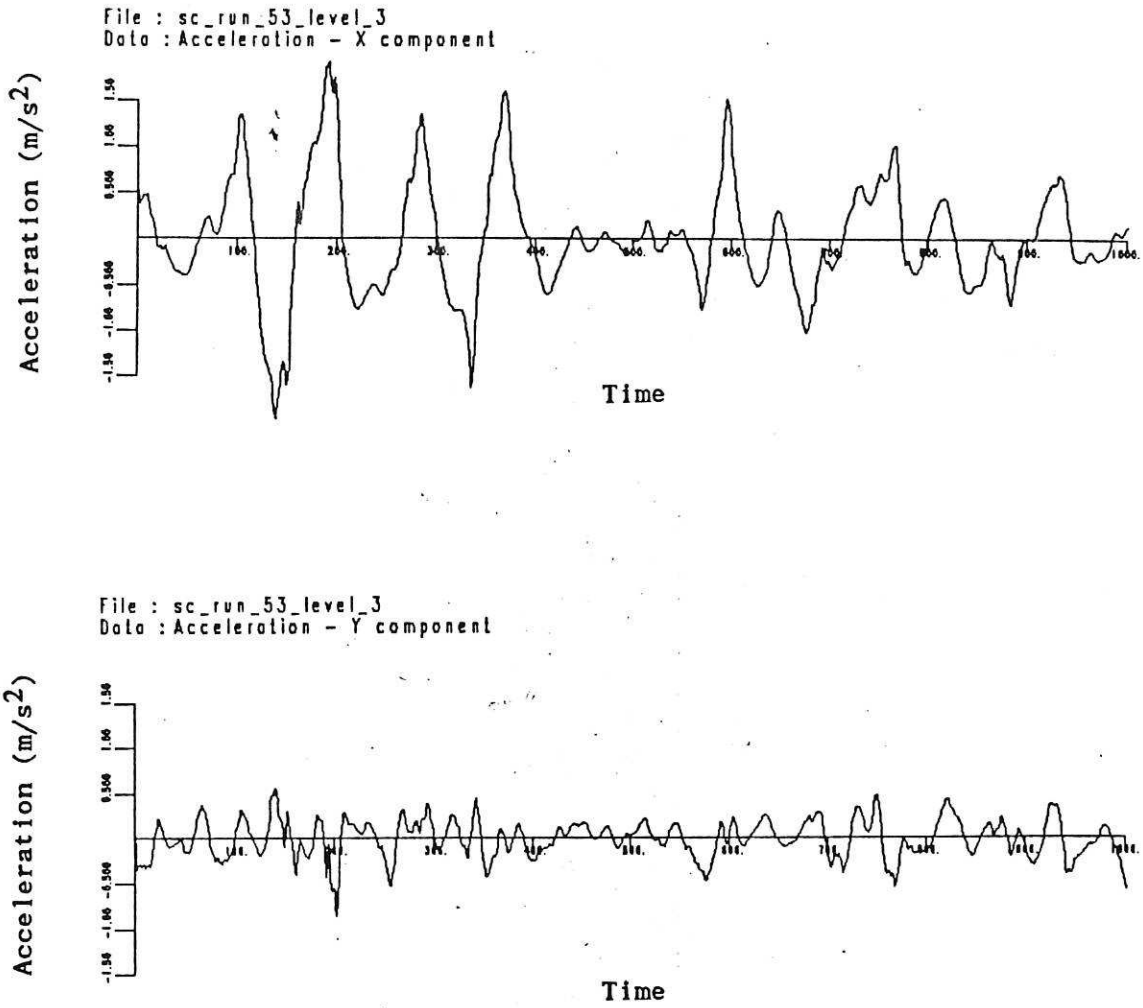

Figure 10. Acceleration components in X and Y directions for sample of Christchurch Bay data.

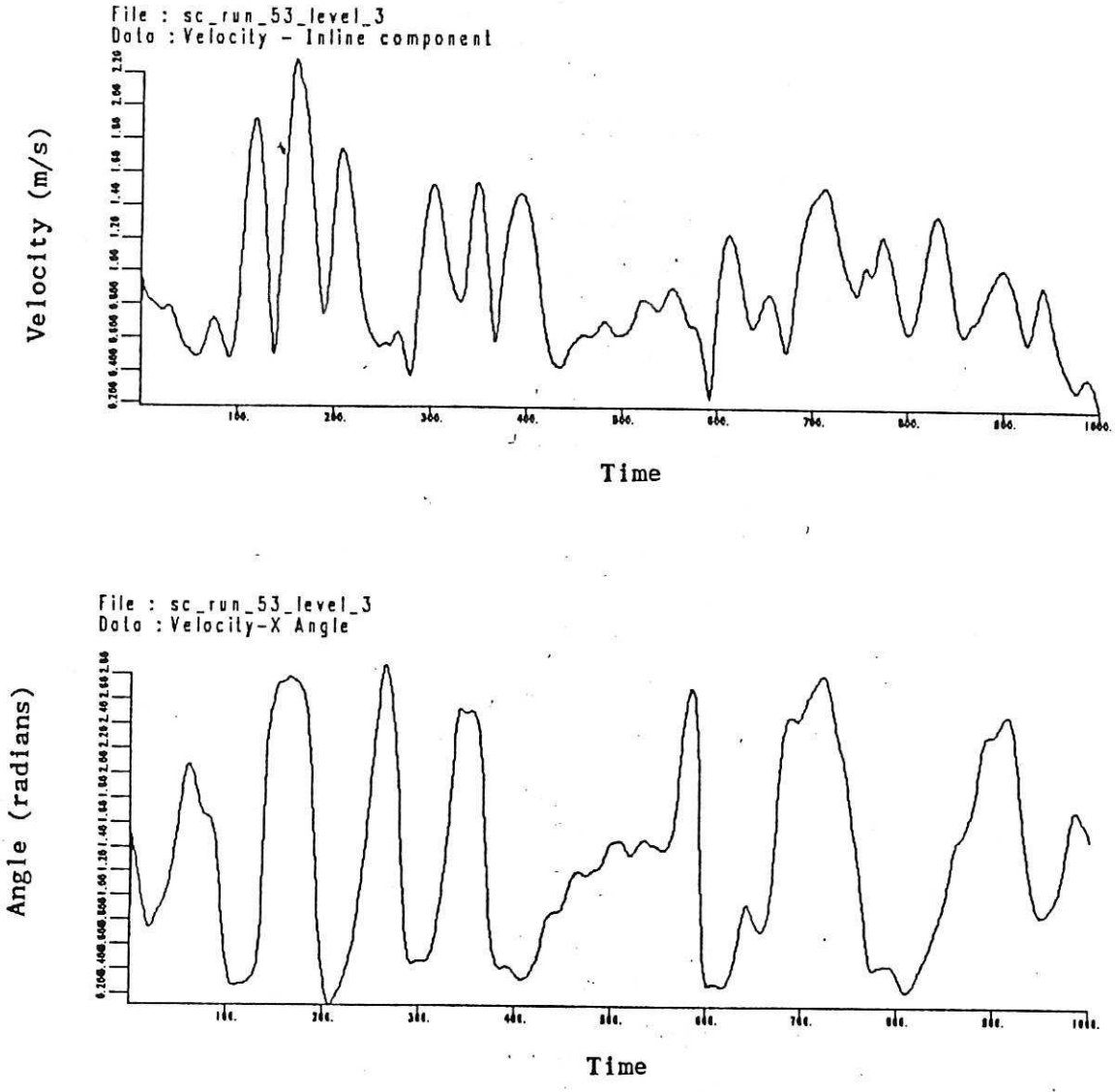

Figure 11. Magnitude of velocity signal and angle between velocity vector and X direction for sample of Christchurch Bay data.

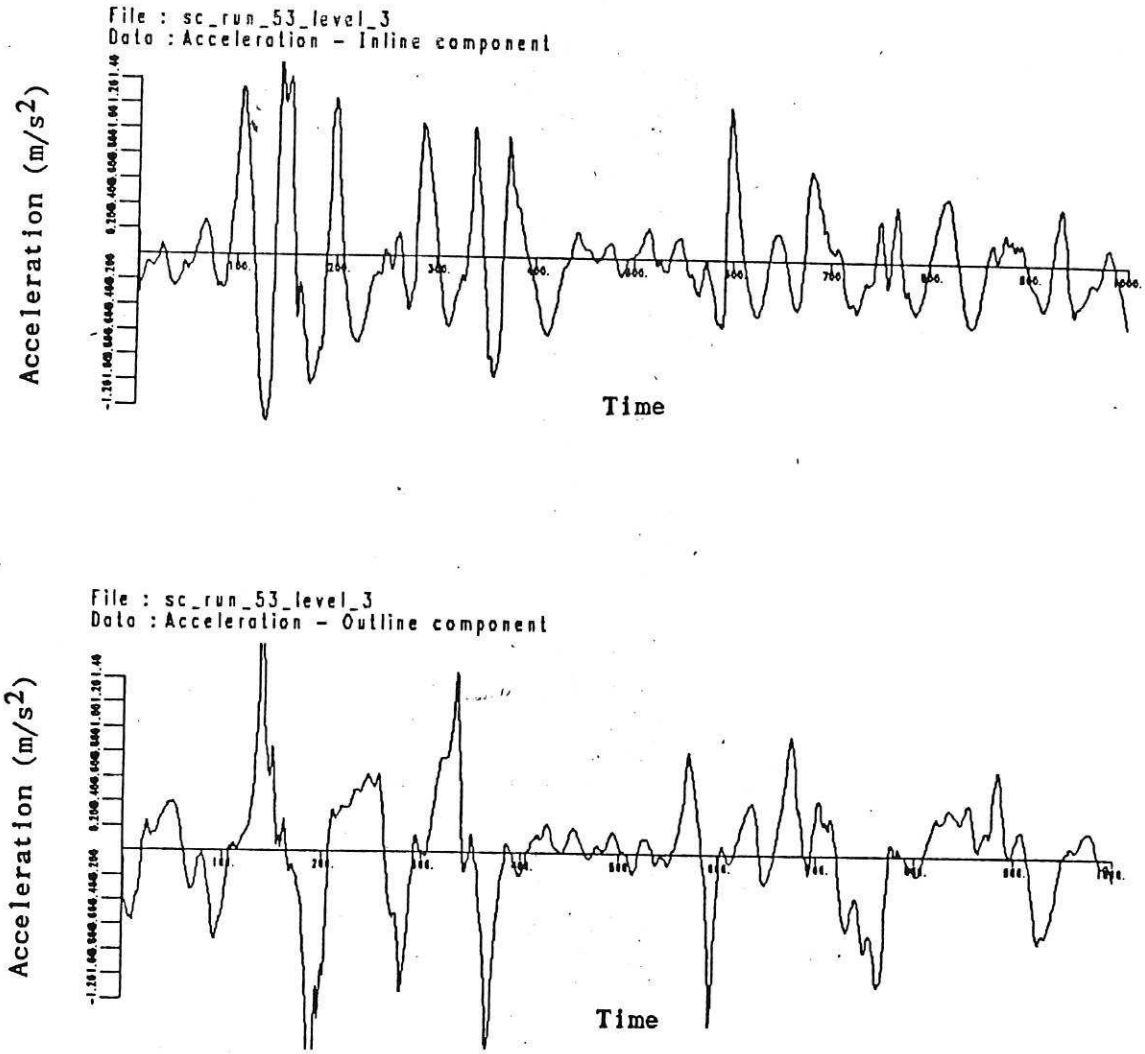

Figure 12. Acceleration components in velocity direction and normal to velocity direction for sample of Christchurch Bay data.

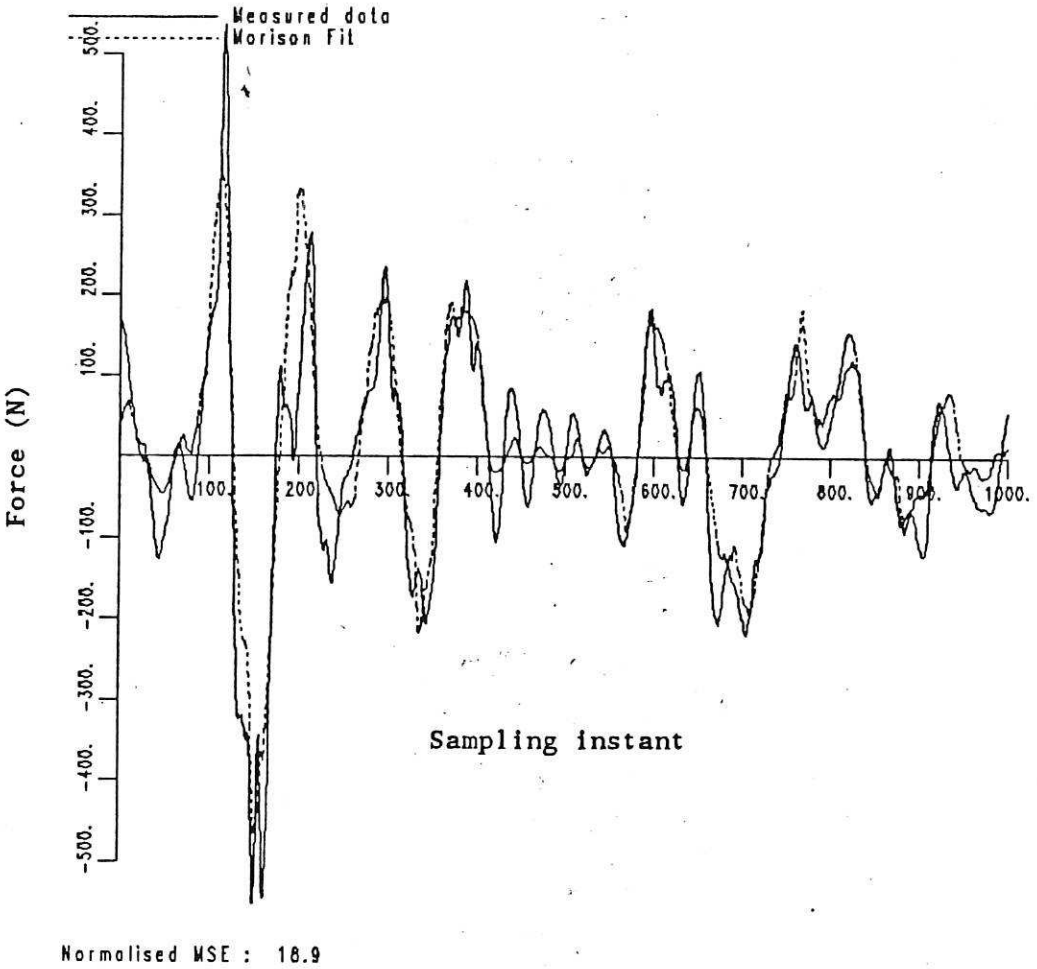

Figure 13. Morison fit to X-direction force for sample of Christchurch Bay data.

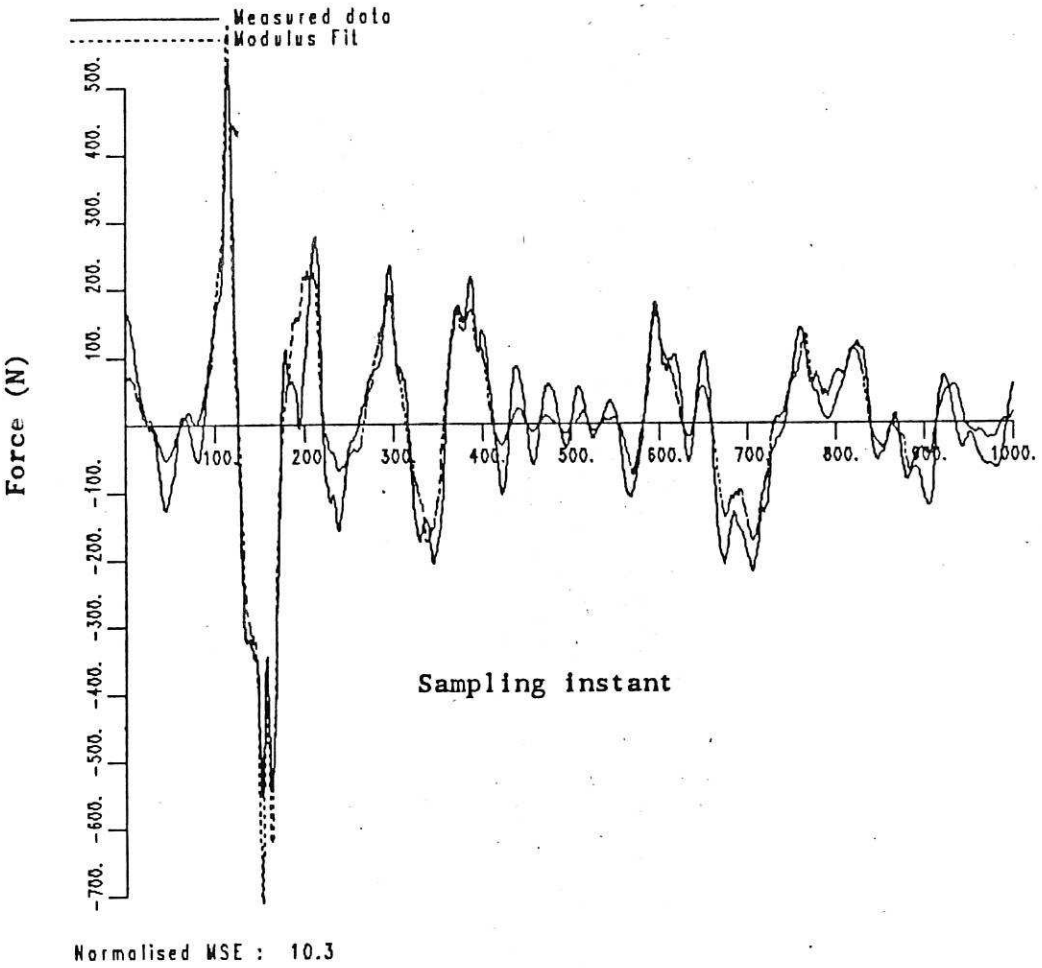

Figure 14. Morison + $\alpha F|F|$ fit to X-direction force for sample of Christchurch Bay data.

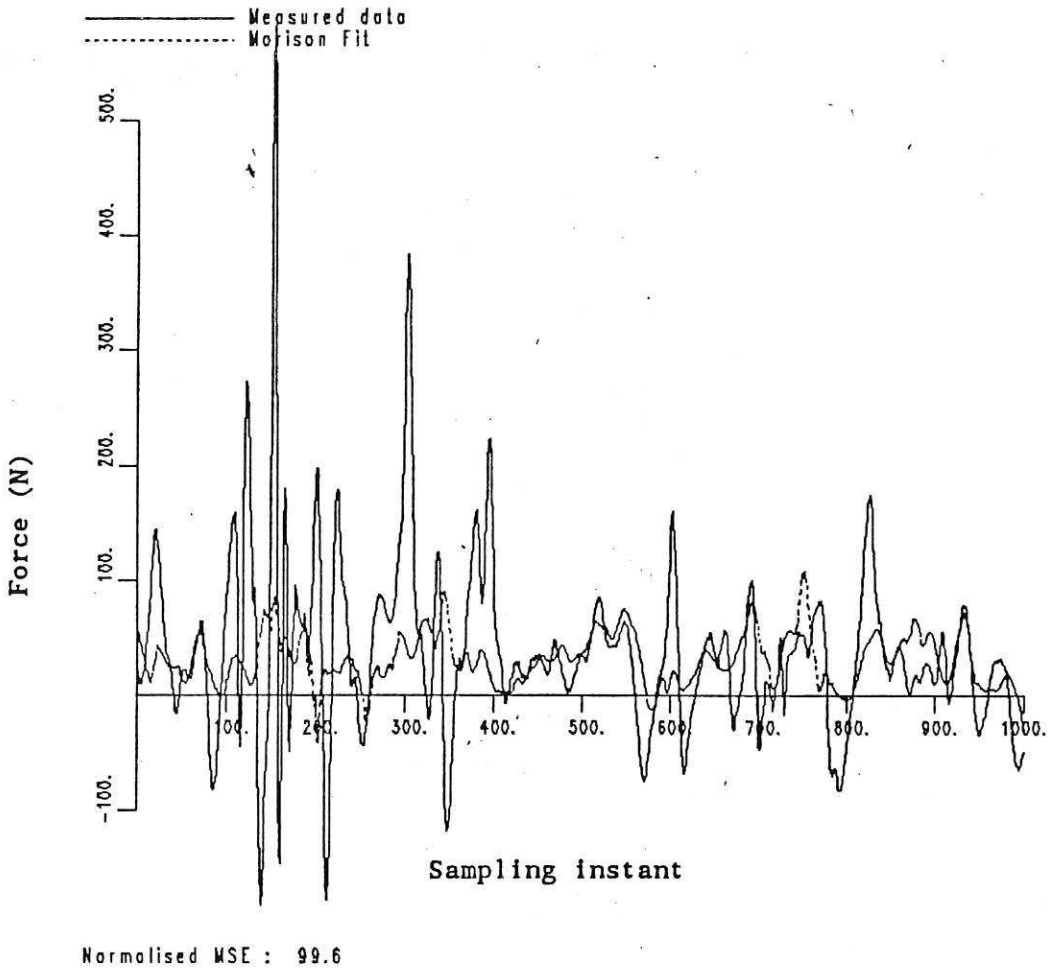

Figure 15. Morison fit to Y-direction force for sample of Christchurch Bay data.

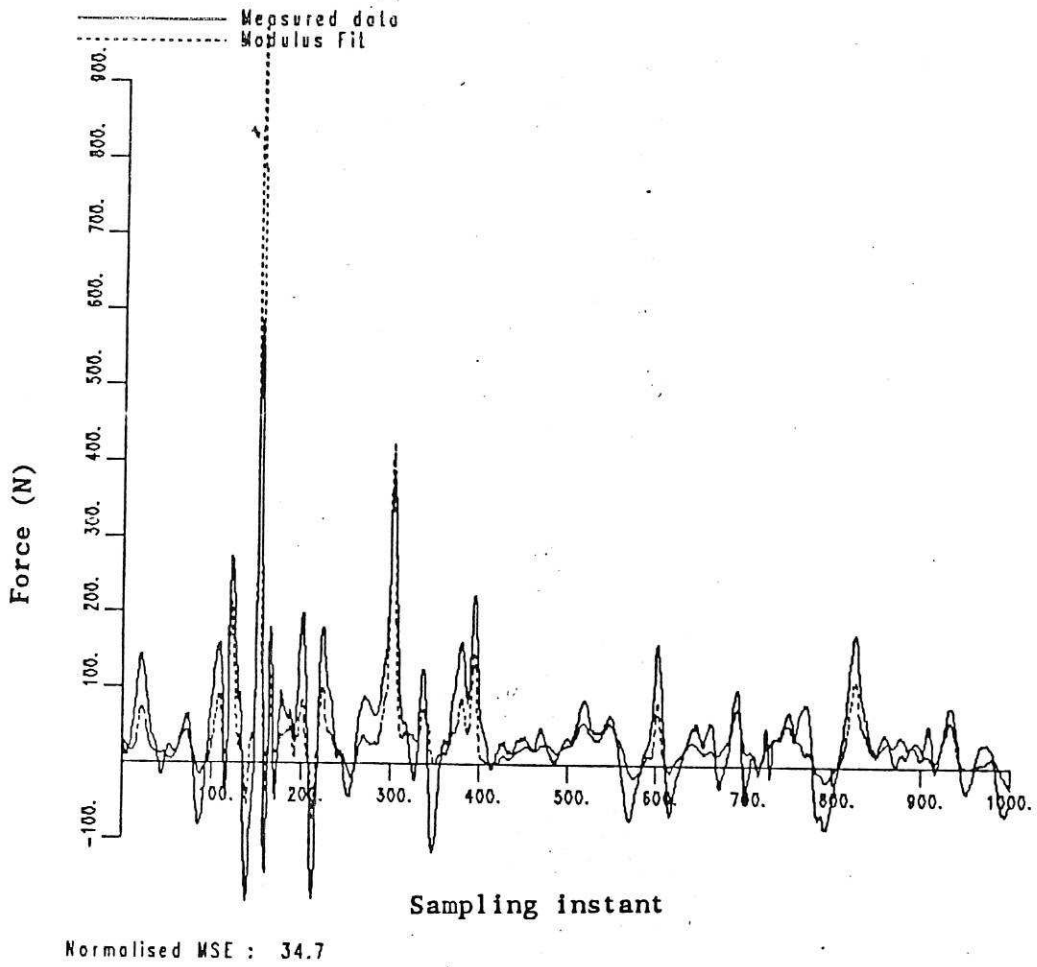

Figure 16. Morison + $\alpha F|F|$ fit to Y-direction force for sample of Christchurch Bay data.

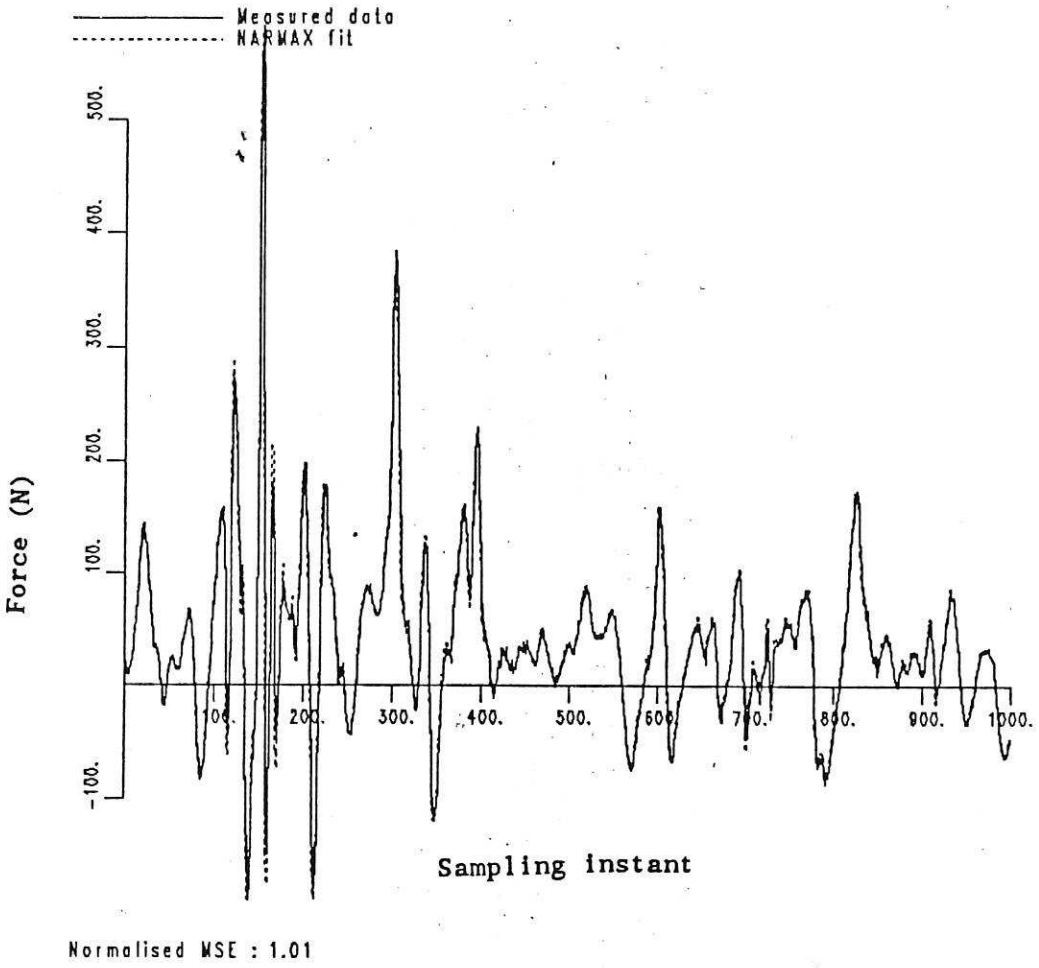

Figure 17. Duffing/Morison fit to Y-direction force for sample of Christchurch Bay data.

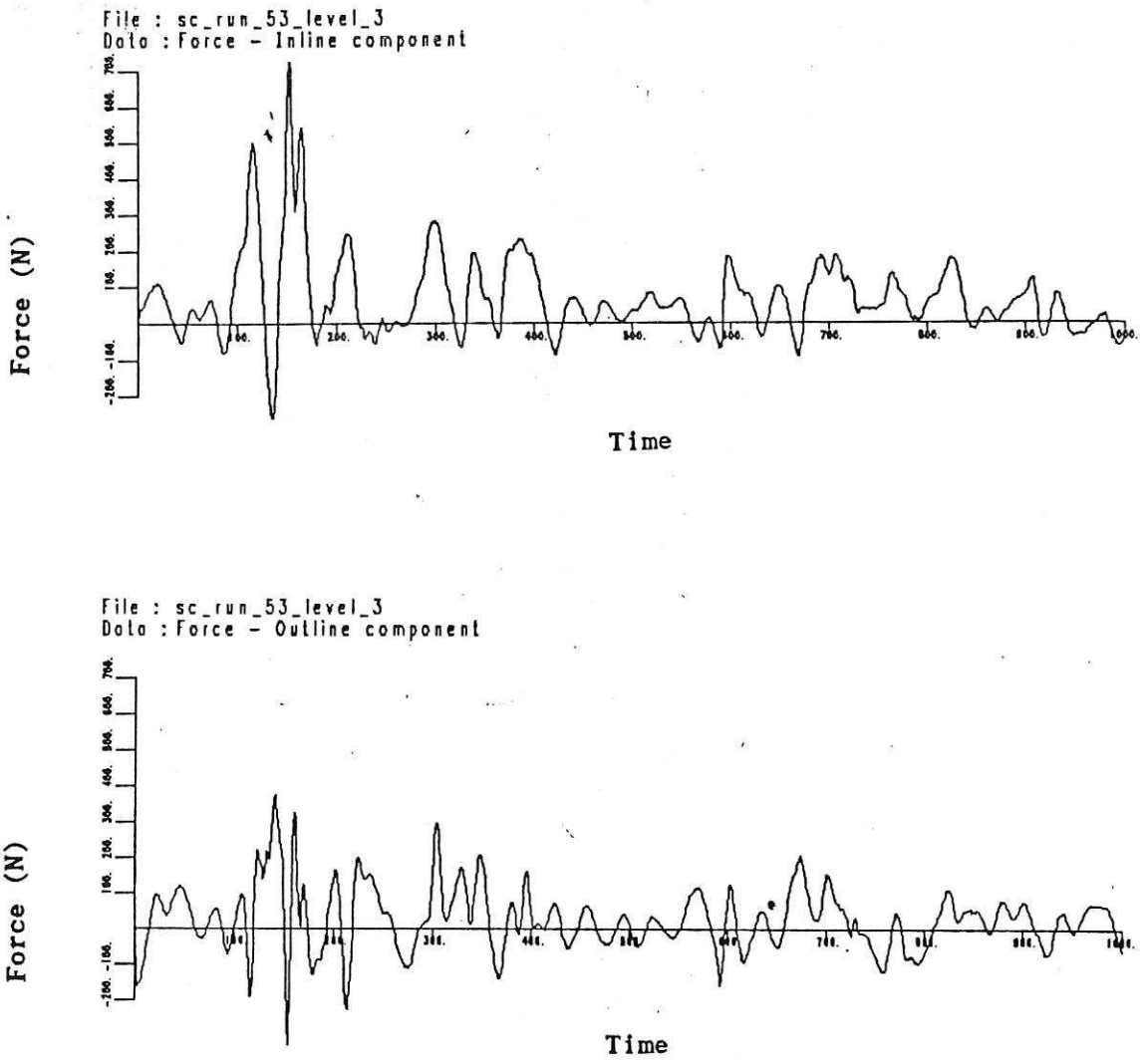

Figure 18. Force components in instantaneous velocity direction and normal to velocity direction for sample of Christchurch Bay data.

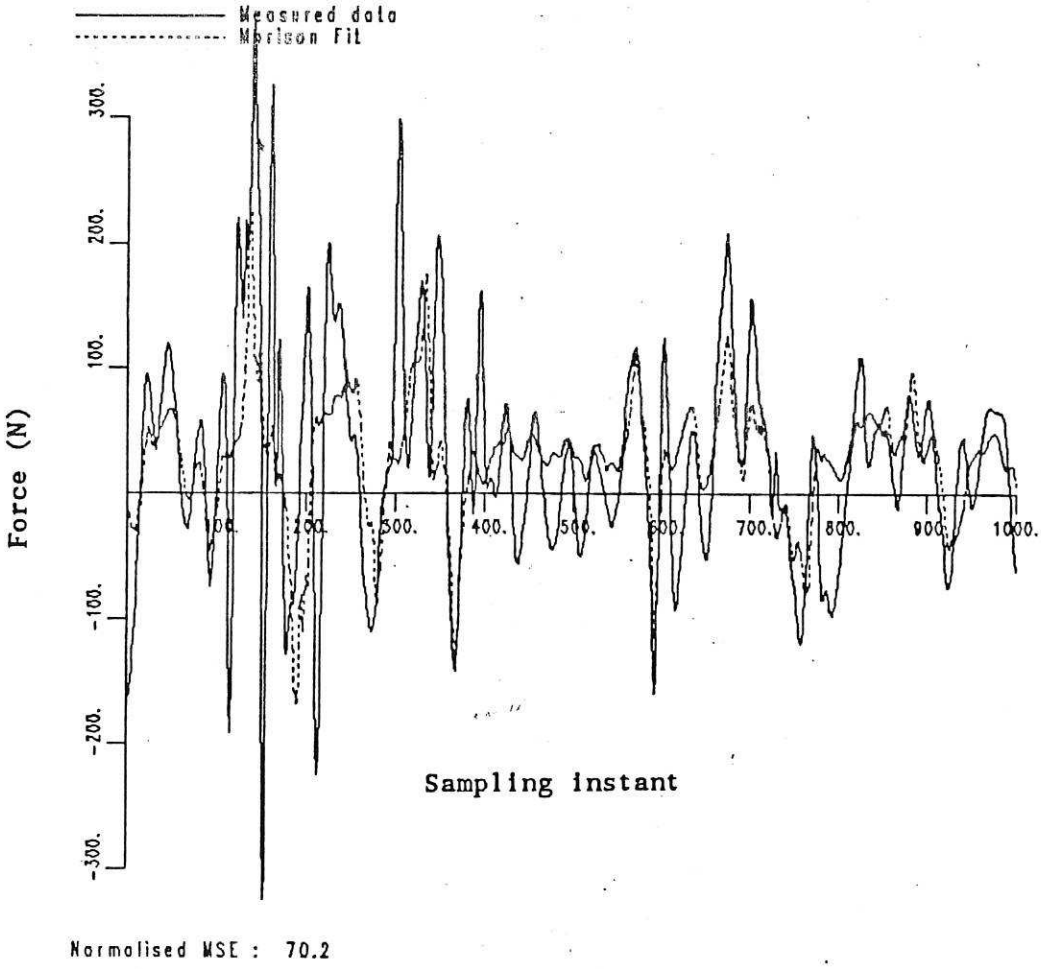

Figure 19. Morison fit to 'out-of-line' force for sample of Christchurch Bay data.

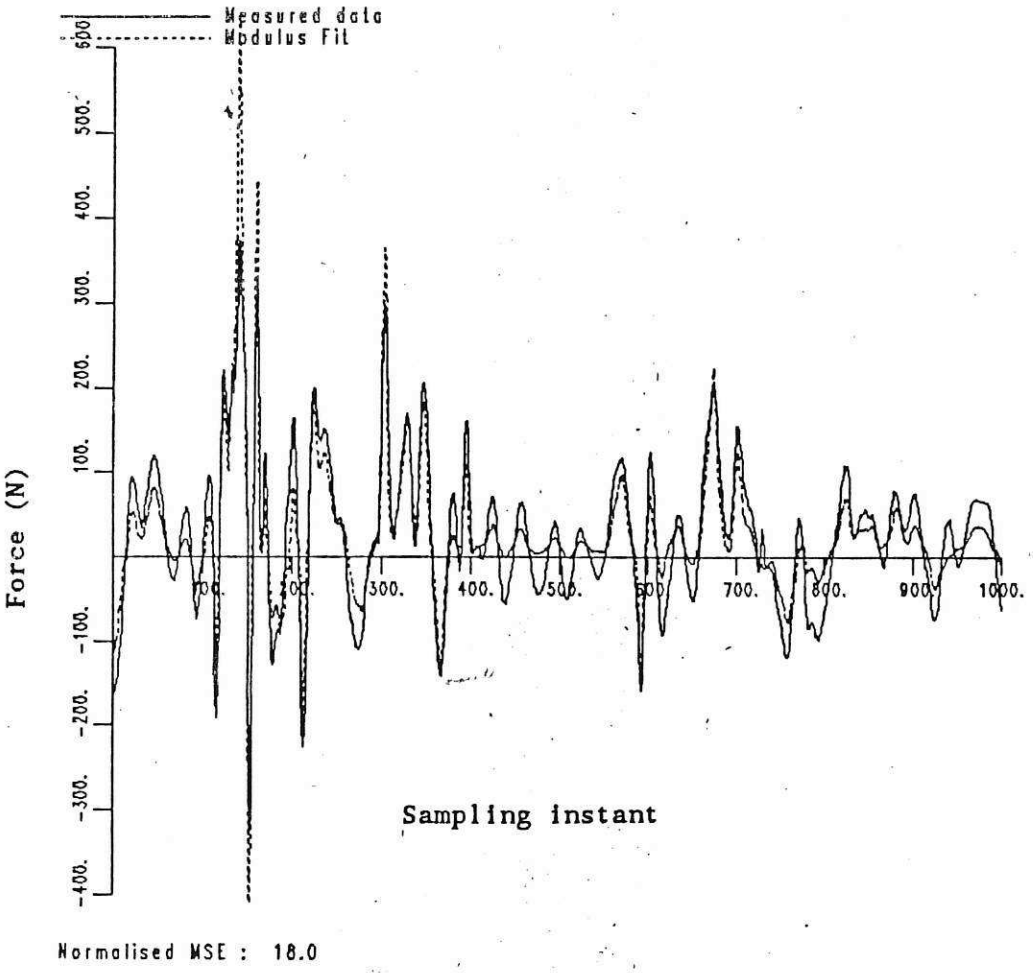

Figure 20. Morison + $\alpha F|F|$ fit to 'out-of-line' force for sample of Christchurch Bay data.